

Simplified Mode-Matching Techniques for the Analysis of Coaxial-Cavity-Coupled Radial E -Plane Power Dividers

Marek E. Bialkowski, *Senior Member, IEEE*, Jens Bornemann, *Senior Member, IEEE*, Vesa P. Waris, *Student Member, IEEE*, and Paul W. Davis

Abstract—Two simplified mode-matching techniques for the numerical analysis of nonsymmetric waveguide E -plane radial N -ports are presented. The first model, which utilizes cartesian and cylindrical coordinate systems for interfacing rectangular waveguides to a coaxial cavity, shows excellent agreement between measurements and computer-intensive finite-element calculations. The second technique, which is based on rectangular coordinates only and thereby neglects the curvature of the coaxial cavity, achieves agreement only for transmission coefficients if the inner radius of the coaxial cavity is sufficiently large. The software for both models are operational on personal computers and require only seconds for a complete analysis. Examples are presented for a Ku-band E -plane six-port and a W-band E -plane ratrace ring. Some additional investigations on the ratrace configuration demonstrate the applicability of the models with respect to reliable component design.

I. INTRODUCTION

WAVEGUIDE components consisting of radial or coaxial cavities with E -plane rectangular waveguide interfaces find applications in many microwave systems. The well-known ratrace hybrid consisting of a coaxial cavity and four waveguide ports is one typical example [1]. Recently, symmetric N -ports formed by a radial or coaxial cavity and E -plane connected rectangular waveguides have been investigated. When impedance is matched, these symmetric N -ports exhibit properties such as constant power division and constant phase difference between different waveguide ports over a relatively large frequency range and, therefore, can be exploited in power combiner and divider applications [2]. More recently, it has been demonstrated that these components can be used to construct microwave and millimeter-wave six-port network analyzers [3], [4].

In order to obtain a predictable and timely design of radial waveguide N -ports, the design engineer has to rely on suitable computer-aided analysis techniques. Computer algorithms restricted to the analysis of symmetric N -ports have been presented in [5] and [6]. In [5], a nonstandard but highly efficient mode-matching technique is used, whereas in [6], a

computer-intensive least-squares boundary residual method is applied. Both methods solve for the scattering parameters of a symmetric N -port. For nonsymmetric radial N -ports, such as the waveguide ratrace ring, however, efficient and accurate analysis algorithms are not yet available.

Therefore, this paper focuses on two simplified mode-matching techniques for the analysis of nonsymmetric coaxial-cavity-coupled radial E -plane power dividers. First, the efficient analysis technique of [5] is extended to cover cases involving nonsymmetric radial E -plane N -ports. In parallel with this nonstandard mode-matching technique, an alternative method, which ignores the curvature of the radial cavity, is described. This second technique assumes straight sections of rectangular waveguides between standard E -plane T -junctions. In order to form a closed structure, i.e., the coaxial cavity, the ends of the configuration obtained by cascading N T -junctions are connected via a hypothetical waveguide section of vanishing length.

II. THEORY

A. Nonstandard Mode-Matching Technique (NS-MMT)

This method is labeled nonstandard because transverse electric and magnetic field components are matched at different interfaces. Together with the utilization of the TE_{1n}^x -mode spectrum instead of a full TE-TM-mode set in [6], this leads to an easy-to-implement algorithm whose main advantage over [6] is its computational speed while maintaining accuracy. The fundamental steps for the extension of this method to the modelling of nonsymmetric N -ports are shown below. For details, the reader is referred to [5].

Fig. 1 shows the geometry. The transverse electromagnetic field components H_x^i and E_ϕ^i in ports $i = 1$ to N are derived from the x components of vector potentials \vec{A}_h

$$H_x^i = \frac{k_c^2}{j\omega\mu_0} A_{hx}^i = \frac{k_c^2}{j\omega\mu_0} \sin\left(\frac{\pi}{a}x'\right) \left\{ \frac{\delta_{1i}}{jk_{z0}^i} e^{-jk_{z0}^i z'} - \sum_{l=0}^L \frac{A_l^i \cos\left(\frac{l\pi}{b}y'\right)}{jk_{zl}^i \sqrt{1 + \delta_{0l}}} e^{jk_{zl}^i z'} \right\} \quad (1)$$

Manuscript received July 26, 1994; revised April 24, 1995.

M. Bialkowski, V. Waris, and P. Davis are with the Department of Electrical and Computer Engineering, The University at Queensland, Queensland 4072, Australia.

J. Bornemann is with the Laboratory for Lightwave Electronics, Microwaves and Communications (LLiMiC), Department of Electrical and Computer Engineering, University of Victoria, Victoria B.C. Canada V8W 3P6.

IEEE Log Number 9412670.

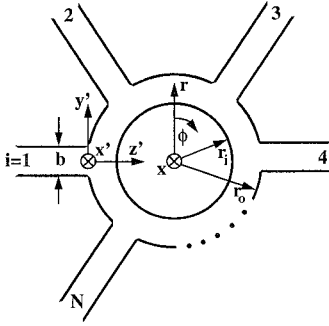


Fig. 1. Coaxial-cavity-coupled radial E -plane waveguide N -port.

with

$$k_c^2 = \omega^2 \mu_0 \epsilon_0 - (\pi/a)^2 \quad (k_{z'l}^2)^2 = k_c^2 - (l\pi/b)^2 \quad (2)$$

δ_{ik} is the Kronecker's delta, and a is the constant width in x ($= x'$) direction. For each port, the H_x component of (1) is matched to that of the coaxial cavity

$$H_x^C = \frac{k_c^2}{j\omega\mu_0} \sin\left(\frac{\pi x}{a}\right) \sum_{m=-M/2}^{M/2} A_m^C e^{jm\phi} T_m(k_c r) \quad (3)$$

over the rectangular aperture at $z' = 0$.

$$H_x^i = H_x^C \quad \text{at} \quad -\frac{b}{2} \leq y' \leq \frac{b}{2} \quad \text{for} \quad i = 1, 2, \dots, N. \quad (4)$$

In (3), the cross-section function is given by

$$T_m(k_c r) = \frac{J_m(k_c r) Y_m'(k_c r_i) - Y_m(k_c r) J_m'(k_c r_i)}{J_m'(k_c r_o) Y_m'(k_c r_i) - Y_m(k_c r_o) J_m'(k_c r_i)} \quad (5)$$

where J and Y are Bessel functions of the first and second kind, respectively, and the prime denotes the derivative with respect to the argument.

The transverse electric field E_ϕ is matched at the outer cavity boundary, i.e., at $r = r_o$

$$E_\phi^C = \begin{cases} \sum_{i=1}^N E_\phi^i & \text{for } \phi^i - \frac{\phi_0}{2} \leq \phi \leq \phi^i + \frac{\phi_0}{2} \\ 0 & \text{otherwise} \end{cases} \quad (6)$$

where in the coaxial cavity

$$E_\phi^C = \sin\left(\frac{\pi x}{a}\right) \sum_{m=-M/2}^{M/2} A_m^C e^{jm\phi} T_m'(k_c r). \quad (7)$$

On those parts of the boundary intersecting the rectangular waveguides, the electric field is given by

$$E_\phi^i = \frac{\partial A_i^z}{\partial r} = \sin\left(\frac{\pi x'}{a}\right) \left(\cos \tilde{\phi}^i e^{-jk_{z_0}^i(z_0 - r \cos \tilde{\phi}^i)} + \sum_{l=0}^L A_l^i \left[\frac{l\pi/b}{jk_{z_l}^i} \sin\left(\frac{l\pi}{b} r \sin \tilde{\phi}^i\right) \sin \tilde{\phi}^i + \cos\left(\frac{l\pi}{b} r \sin \tilde{\phi}^i\right) \cos \tilde{\phi}^i \right] e^{jk_{z_0}^i(z_0 - r \cos \tilde{\phi}^i)} \right) \quad (8)$$

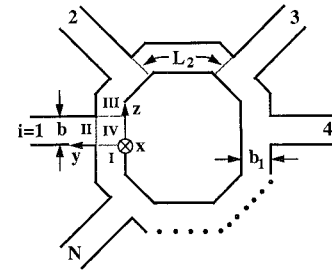


Fig. 2. Geometry considered for the straight-waveguide mode-matching technique (bends neglected).

where abbreviations

$$y' = r \sin(\phi - \phi^i) = r \sin \tilde{\phi}^i \quad (9)$$

$$z' = r_o \cos(\phi_0/2) - r \cos(\phi - \phi^i) = z_0 - r \cos \tilde{\phi}^i \quad (10)$$

are used. The matching conditions of the coaxial cavity to the N rectangular waveguides are given by (4) and (6). After multiplying these equations with the appropriate orthogonal functions and integrating over the intervals $0 \leq \phi \leq 2\pi$ in (6) and $-b/2 \leq y' \leq b/2$ in (4), an algebraic set of equations for unknown coefficients $\{A_i^i\}$ is obtained. This system of equations is solved and the scattering parameters of the N -port are determined. Note that the use of the rectangular boundary $-b/2 \leq y' \leq b/2$ in setting the algebraic equation for $\{A_i^i\}$, requires the evaluation of functions $T_m(k_c r)$ at $r = r_o$. This was one of the reason for using approximations of T_m in [5].

In order to avoid these approximations, the boundary condition for H_x can be set at $r = r_o$ for $\phi^i - \phi_0/2 \leq \phi \leq \phi^i + \phi_0/2$. The weighting functions to multiply equations for H_x are of the form $\cos\{k\pi(\phi + \phi^i)/\phi_0\}$. The last manipulation obviates the need for approximations of cylindrical functions used in [5]. The calculations have shown that the old method and the newly proposed method of generating equations for unknown coefficients $\{A_i^i\}$ produced equally accurate results.

B. Straight-Waveguide Mode-Matching Technique (SW-MMT)

The geometry for the straight-waveguide mode-matching technique, which is based on cascaded E -plane T -junctions, is depicted in Fig. 2. Note that the bends in waveguide b_1 (shown here as 45-degree bends) are neglected in this model. Since the rectangular E -plane T -junction is well documented in literatures, e.g. [1], [7], it is, in many cases, less time-consuming to cascade T -junction modules rather than developing an entirely new algorithm. Therefore, it was considered appropriate to compare this approach with the nonstandard mode-matching technique and to demonstrate its limitations.

As in the nonstandard mode-matching technique, the electromagnetic field in each of the three ports connected to an individual T -junction is derived from the x component of a vector potential involving wave-propagating terms for regions $\nu = \text{I, II, III}$ and cross-section functions

$$T_n^\nu(x, y, z) = A_n^\nu \frac{\sin\left(\frac{\pi x}{a}\right)}{\sqrt{1 + \delta_{0n}}} \begin{cases} \cos \frac{n\pi}{b_1} y & \nu = \text{I, III} \\ \cos \frac{n\pi}{b} z & \nu = \text{II} \end{cases} \quad (11)$$

In the resonator region IV, the respective expression is a superposition of cross-section functions

$$A_{h,x}^{IV} = \sum_i T_i^{IV,I} + \sum_k T_k^{IV,II} + \sum_m T_m^{IV,III} \quad (12)$$

where

$$T_i^{IV,I}(x, y, z) = C_i^I \sin\left(\frac{\pi}{a}x\right) \frac{\cos\left(\frac{i\pi}{b_1}y\right)}{\sqrt{1 + \delta_{0i}}} \cos\{k_{zi}^I(z - b)\} \quad (13)$$

$$T_k^{IV,II}(x, y, z) = C_k^{II} \sin\left(\frac{\pi}{a}x\right) \frac{\cos\left(\frac{k\pi}{b}z\right)}{\sqrt{1 + \delta_{0k}}} \cos(k_{yk}^{II}y) \quad (14)$$

$$T_m^{IV,III}(x, y, z) = C_m^{III} \sin\left(\frac{\pi}{a}x\right) \frac{\cos\left(\frac{m\pi}{b_1}y\right)}{\sqrt{1 + \delta_{0m}}} \cos(k_{zm}^{III}z) \quad (15)$$

and k_z^I , k_y^{II} , k_z^{III} are the propagation constants in regions I, II, III, respectively. For a detailed derivation of the E -plane T -junction, the reader is referred to [1]. Matching the transverse electric and magnetic fields at the three interfaces leads to the generalized scattering matrix of the T -junction with only a single matrix inversion [7]. The connecting length to the following junction is represented by diagonal matrices

$$\mathbf{R} = \text{diag}\{\exp(-jk_{zn}^{III}L_i)\} \quad (16)$$

which are cascaded with the T -junction submatrices \mathbf{S}_{ik} to form the generalized scattering matrix of the module: T -junction plus following assumed straight waveguide of length L_i

$$\mathbf{S} = \begin{bmatrix} \mathbf{S}_{11} & \mathbf{S}_{12} & \mathbf{S}_{13}\mathbf{R} \\ \mathbf{S}_{21} & \mathbf{S}_{22} & \mathbf{S}_{23}\mathbf{R} \\ \mathbf{R}\mathbf{S}_{31} & \mathbf{R}\mathbf{S}_{32} & \mathbf{R}\mathbf{S}_{33}\mathbf{R} \end{bmatrix}. \quad (17)$$

For each port $i = 2$ to N , the individual matrix of the form (17) is cascaded using a general algorithm [1] to combine an M -port with a K -port to form an $(M + K - 2)$ -port. Note that the T -junction in this case needs to be calculated only once. Finally, the input port ($\nu = I$) of junction $i = 1$ and the output port ($\nu = III$) of junction $i = N$ are connected by a hypothetical waveguide of vanishing length to simulate the closed structure of the coaxial cavity.

III. RESULTS

Based on the two analyses described above, two Fortran computer algorithms were developed for operation on an IBM PC or compatible. These algorithms were then applied to perform calculations of scattering parameters for a variety of symmetric and nonsymmetric structures incorporating a coaxial cavity and E -plane-connected rectangular waveguides.

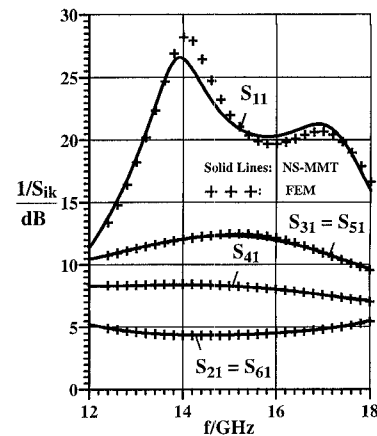


Fig. 3. Comparison between NS-MMT and finite-element analysis (HFSS) results for an example of a symmetric six-port. Dimensions: $a = 2b = 15.8$ mm, $r_i = 4.0$ mm, $b_1 = r_o - r_i = 6.5$ mm; ports spaced at 60° angles.

The advantage of both of the developed algorithms, compared, e.g., to a full-wave TE-TM-mode analysis or finite-element routines, such as Hewlett Packard's High Frequency Structure Simulator (HFSS), is computational speed. For the analysis of a nonsymmetric four-port, e.g., a ratrace ring, at 100 frequency samples, the nonstandard (NS-MMT) and the straight-waveguide (SW-MMT) mode-matching techniques require 70 and 60 seconds, respectively, on a 66 MHz personal computer. For NS-MMT, 25 cavity modes and three waveguide modes have turned out to be sufficient. The respective numbers for SW-MMT are: 15 modes for the T -junction analysis and five modes for cascading individual junctions. In comparison, it takes several hours for HFSS on a SUN IPX workstation to obtain only a few frequency points for the same structure.

The excellent agreement of NS-MMT with results from a finite-element analysis (HFSS) is demonstrated in Fig. 3 for an example of a symmetric six-port in Ku-band. Recognizable maximum differences of 2 dB can only be observed beyond 25 dB return loss, and it is idle to argue in favor of the accuracy of either HFSS or NS-MMT. For the 29 frequency points, shown as FEM analysis, HFSS requires approximately one hour per frequency point on a SUN IPX workstation for an adaptive convergence criterion of $\Delta S = 0.01$ or ten adaptive mesh refinement passes at 18 GHz. In comparison, NS-MMT provides the results for 29 frequency points within 25 seconds on a 66 MHz 486 PC.

The second method investigated, SW-MMT, provides only approximate results for the symmetric six-port, which are not shown here. A major discrepancy between SW-MMT and HFSS is the return loss. This discrepancy stems from the fact that the return loss into the input of the symmetrical six-port is strongly dependent on the presence of the match-loaded ports on the opposite side of the coaxial cavity. Note that the height of the input waveguide h , the cavity height b_1 and the coaxial cavity's inner cylinder of diameter $2r_i$ are of similar dimensions (cf., legend to Fig. 3). Therefore, this situation cannot be properly modelled by the straight waveguide T -junction approach as the opposite wall in this model is assumed perfectly conducting.

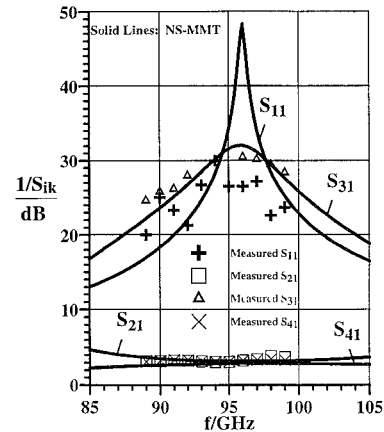
Fig. 4 shows comparisons with measurements and finite-element results for a 94 GHz E -plane ratrace ring for which simple design guidelines are given in [1]. Considering the limitations of the measurement setup and even neglecting the influence of mechanical tolerances and ohmic losses, good agreement is observed below 20 dB for NS-MMT [Fig. 4(a)]. In order to investigate the nature of the discrepancies in the region above 20 dB, HFSS results were produced and are shown in Fig. 4(b). Very good agreement between NS-MMT and HFSS is obtained. This comparison leads to the conclusion that the discrepancies observed in Fig. 4(a) could be due to measurement uncertainties and/or mechanical tolerances, which can easily occur in this millimeter-wave frequency range. In Fig. 4(c), except for the disagreement in return loss, which follows the reasoning given in the previous paragraph, good results are obtained for the transmission coefficients calculated using SW-MMT. The better agreement between SW-MMT, HFSS and measured results is believed to be due to a smaller number of ports as well as the nonsymmetric configuration of the ratrace hybrid: Two ports see a conducting wall on the opposite side of the coaxial cavity. In this way, the approximation of the coaxial cavity by the straight-waveguide T -junction model is better justified than for the symmetric six-port.

Tuning possibilities by varying the inner radius r_i of an E -plane ratrace ring are investigated in Fig. 5 (NS-MMT results only). Comparing Fig. 5(a) with Fig. 4(a), it is obvious that an increase in r_i reduces the operating frequency and increases the isolation (S_{31}). At the same time, however, the return loss deteriorates since the metallic surface at r_i now more efficiently blocks the apertures of the waveguide ports. This effect limits the tuning range towards lower frequencies. Towards higher frequencies, good isolation and return loss behavior is maintained for decreasing r_i [Fig. 5(b)], but at the expense of a slightly unequal power division.

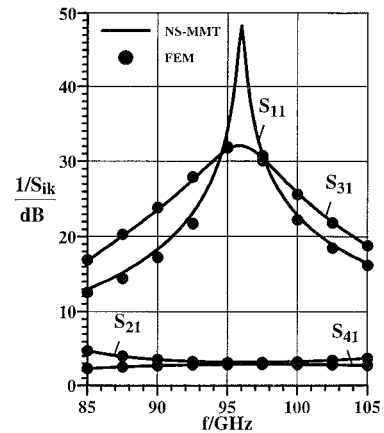
Fig. 6 addresses the fact that the straightforward ratrace ring design can cause substantial fabrication problems due to extremely small inner radii, particularly at millimeter-wave frequencies. Therefore, Fig. 6 shows the performance of the W -band ratrace ring with a 4.5λ pathlength instead of a 1.5λ one. As expected, the operational bandwidth is reduced, and power division and isolation are maintained. However, the increase in pathlength also results in an increase of r_i and, therefore, to a curvature that better resembles the straight-waveguide approach (SW-MMT). Consequently, NS-MMT (solid lines) and SW-MMT (dashed lines) results tend to merge. From a practical standpoint, however, the input return loss degrades considerably due to the larger curvature of the 4.5λ ring.

IV. CONCLUSION

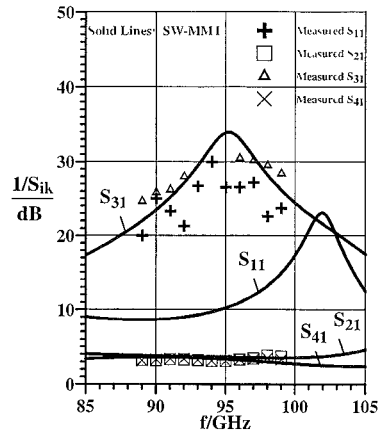
Two simplified mode-matching techniques for the analysis of nonsymmetric radial waveguides, which are E -plane-coupled via a coaxial cavity, are presented. Both techniques provide results considerably faster than other methods known so far and are operational on standard personal computers. By comparison with data from a finite-element analysis and



(a)



(b)



(c)

Fig. 4. Comparison of theoretical results with measurements of a W -band waveguide ratrace ring. Dimensions: $a = 2b = 2.54$ mm, $r_i = 0.513$ mm, $b_1 = 0.898$ mm; ports at 0° (1), 60° (2), 120° (3), 180° (4). (a) NS-MMT. (b) HFSS. (c) SW-MMT.

measurements, it is demonstrated that, by virtue of its computational speed and accuracy, the nonstandard mode-matching technique (NS-MMT) is the preferred choice for the design of radial waveguide power dividers. Within its limitations and for reasonably large curvatures, the straight-waveguide mode-matching technique (SW-MMT) can be applied as a first-order approximation. Theoretical investigations of a W -band ratrace ring explain the influence of the cavity radius with respect

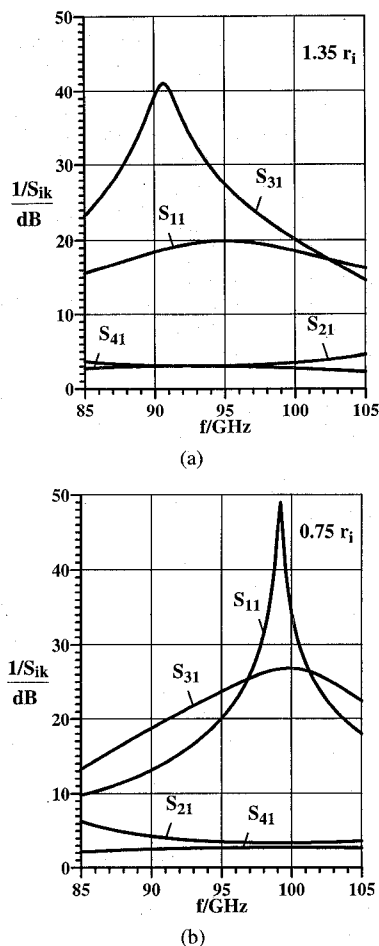


Fig. 5. NS-MMT results for variation of inner radius. Dimensions as in Fig. 4, except (a) inner radius equals 1.35 times that of Fig. 4, (b) inner radius equals 0.75 times that of Fig. 4.

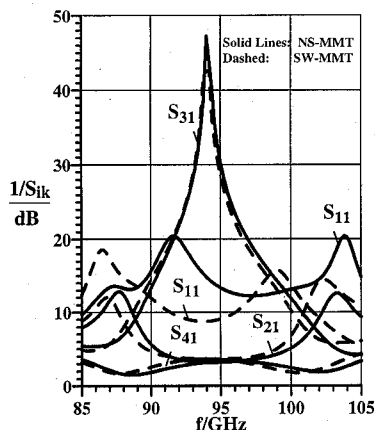


Fig. 6. Comparison of NS-MMT (solid lines) and SW-MMT (dashed lines) for 4.5λ W-band waveguide ratrace ring. Dimensions as in Fig. 4, except $r_i = 3.384$ mm.

to component performance and the two different modelling strategies.

ACKNOWLEDGMENT

The authors are greatly indebted to Deutsche Aerospace Ulm, Germany, for providing the measured data of the W-band

ratrace ring (originally released in Final Report 'Studie 94 GHz Leistungsendstufen' Contract TR/R624/D0064/D2660). In particular, the authors would like to thank Dr. K.-E. Schmegner of Deutsche Aerospace Ulm for helpful suggestions and discussions.

REFERENCES

- [1] J. Uher, J. Bornemann, and U. Rosenberg, *Waveguide Components for Antenna Feed Systems. Theory and CAD*. Norwood: Artech House, 1993.
- [2] A. L. Cullen and S. P. Yeo, "Designing a symmetrical five-port waveguide junction," *IEE Proc.-H*, vol. 135, no. 1, pp. 17–22, 1988.
- [3] G. P. Riblet, "An E-plane coupled matched waveguide 5-port for making 6-port measurements," in *1983 IEEE MTT-S Int. Microwave Symp. Dig.*, pp. 272–274.
- [4] K. Chang, M. Li, and K. A. Hummer, "High-power four-way power divider/combiner," in *1990 IEEE MTT-S Int. Microwave Symp. Dig.*, pp. 1329–1332.
- [5] M. Bialkowski, "Analysis of an N-port consisting of a radial cavity and E-plane coupled rectangular waveguides," *IEEE Trans. Microwave Theory Tech.*, vol. 40, pp. 1840–1843, Sept. 1992.
- [6] A. L. Cullen and S. P. Yeo, "Using the least-squares boundary residual method to model the symmetrical five-port waveguide junction," *IEE Proc.-H*, vol. 134, no. 2, pp. 116–124, 1987.
- [7] T. Sieverding and F. Arndt, "Field theoretic CAD of open or aperture matched T-junction-coupled rectangular waveguide structures," *IEEE Trans. Microwave Theory Tech.*, vol. 40, pp. 353–362, Feb. 1992.



Marek E. Bialkowski (SM'88) received the M.Eng.Sc. degree in 1974 in applied mathematics and the Ph.D. degree in 1979 in electrical engineering, both from the Warsaw Technical University, Poland.

In 1979, he became an Assistant Professor at the Institute of Radioelectronics, Warsaw Technical University. In 1981, he was awarded a Postdoctoral Research Fellowship by the Irish Department of Education and spent one year at the University College Dublin carrying out research in the area of microwave circuits. In 1982, he won a Postdoctoral Research Fellowship from the University of Queensland, Brisbane, Australia. During his stay in Brisbane he worked on the modeling of millimeter-wave guiding structures (particularly on waveguide diode mounts). In 1984, he joined the Department of Electrical and Electronic Engineering, James Cook University, Townsville, Australia, as a Lecturer in the field of communications. In 1986 he was promoted to Senior Lecturer. In 1988, he was a Visiting Lecturer in the Department of Electronics and Computer Science, University of Southampton, U.K. He was invited to lecture in the field of antenna theory and design. In 1989, he accepted an appointment as Reader (Associate Professor) in Communications and Electronics in the Department of Electrical Engineering at the University of Queensland, Brisbane, Australia. At present he is the leader of the Microwave and Antenna Group there. In 1994, he held an appointment as a Visiting Professor in the Department of Electrical and Computer Engineering in the University of Victoria, Victoria, Canada. His current research interests include computational electromagnetics, six-port techniques, quasi-optical power combining techniques, antennas for mobile satellite communications, low profile antennas for reception of satellite broadcast TV programs, near-field/far-field antenna measurements and industrial applications of microwaves.

Dr. Bialkowski is a member of the Editorial Board for the IEEE TRANSACTIONS ON MICROWAVE THEORY AND TECHNIQUES. Also, he is a member of the Editorial Board for the *Asia-Pacific Engineering Journal*. His name is listed in *Marquis Who's in the World* (USA), *Who's Who in Science and Engineering* (USA), *Dictionary of International Biography* (IBC, UK), *Men of Achievement* (IBC, UK), and *International Who's Who of Contemporary Achievement* (ABI, USA).

Jens Bornemann (M'87–SM'90), for a photograph and biography, see this issue, p. 1787.



Vesa P. Waris (S'91) was born in Pello, Finland in 1967. He received the B.E. degree from the University of Queensland in 1988. He is currently completing his Ph.D. at the University of Queensland, researching power combiners and dividers.

Since 1989 he has worked for MITEC Ltd. as a Design Engineer, with projects including the *L*-band Radioastron receiver, phase-locked oscillators, a 30 GHz receiver using packaged HEMT's, and various satellite earth-station equipment.

Mr. Waris is the holder of an Australian Post-

graduate Award.



Paul W. Davis received the B.Eng. (Hons.1) degree in electrical engineering in 1991 from the University of Queensland, Australia. As a graduate, he was awarded the University of Queensland Medal. In 1994 he was awarded an Australian Postgraduate Research Award (Industry), (APRAI), to work towards a Ph.D. degree with the Microwave and Antenna Group at the University of Queensland. His topic is low profile antennas for the reception of direct broadcast satellite television.

From 1992 to 1993, he was employed with the Queensland Electricity Commission as a Communications Engineer in Townsville, Australia. His current research interests include finite element methods, spectral domain methods for analysis of planar transmission lines, mobile and satellite communications.